Theory for Multicomponent Adsorption Equilibrium: Multispace Adsorption Model

Vladimir Gusev and James A. O'Brien
Dept. of Chemical Engineering, Yale University, New Haven, CT 06520

Craig R. C. Jensen and Nigel A. Seaton
Dept. of Chemical Engineering, University of Cambridge, Pembroke Street, Cambridge CB2 3RA, U.K.

A new theory for the prediction of multicomponent adsorption equilibrium in noncrystalline porous solids is presented: the multispace adsorption model (MSAM). This theory allows for the inherent nonuniformity of the adsorbed phase by describing separately the adsorption in "spaces" close to, and far from, the adsorbent surface. The inputs to the calculation are the pure-species adsorption isotherms and a single parameter characteristic of the adsorbent that can be obtained from very limited mixture data. We evaluate the theory by predicting multicomponent adsorption for a range of carbon adsorbents, making use of our own experimental results and literature data. The MSAM gives quantitative predictions for all the systems studied.

Introduction

The design of an adsorptive separation process relies on accurate thermodynamic predictions of multicomponent adsorption. This is the case even for processes that do not closely approach equilibrium, as thermodynamics provides estimates of driving forces for kinetic separations. Unfortunately, the predictions of adsorption thermodynamics are generally less accurate than those of bulk fluid mixture thermodynamics. Perhaps most significantly, unlike in bulk thermodynamics it is difficult to identify in advance systems (i.e., adsorbent/adsorbate mixture combinations) that will be difficult. Thus, the designer of a distillation column can have more confidence in his or her thermodynamics calculations than can the designer of a pressure-swing adsorption process. To some degree, the poorer performance of adsorption thermodynamic models is an inevitable consequence of the presence of an additional substance (i.e., the adsorbent) that has rather complex interactions with the fluid mixture. Nevertheless, because of the importance of adsorptive separations, the development of better models for multicomponent adsorption thermodynamics is a worthwhile goal.

A rigorous description of adsorption from the gas phase is difficult because the adsorbate/gas interfacial region is ill defined. The Gibbsian treatment of adsorption replaces the real system with a hypothetical, yet thermodynamically equivalent, one. Here the gas phase is imagined to extend unchanged up to the solid surface, and the adsorbed phase is described by an imaginary two-dimensional system with its own thermodynamic properties.

We use the term "two-dimensional" because the fundamental property relation for this hypothetical phase is commonly written in terms of the surface area of the adsorbent, A, and the spreading pressure, π:

$$dU = TdS - \pi dA + \sum \mu_i dn_i. \tag{1}$$

In this equation, U and S are, respectively, the internal energy and entropy of the adsorbate; μ_i is the chemical potential; and n_i the number of moles adsorbed of species i. In fact, it is not necessary to view the adsorbed phase as two-dimensional; πdA may be regarded as a generalized work term, requiring no connection with a two-dimensional picture of adsorption; Cracknell and Nicholson (1995) have shown that it can be advantageous to interpret adsorption thermodynamic theories in these terms. The key physical assumption is that the adsorbed phase is uniform, in the sense that each adsorbate molecule experiences the same interaction with the adsorbent, regardless of location. The analogue of the Gibbs–Duhem equation for adsorption is the Gibbs adsorption isotherm:

Correspondence concerning this article should be addressed to J. A. O'Brien.

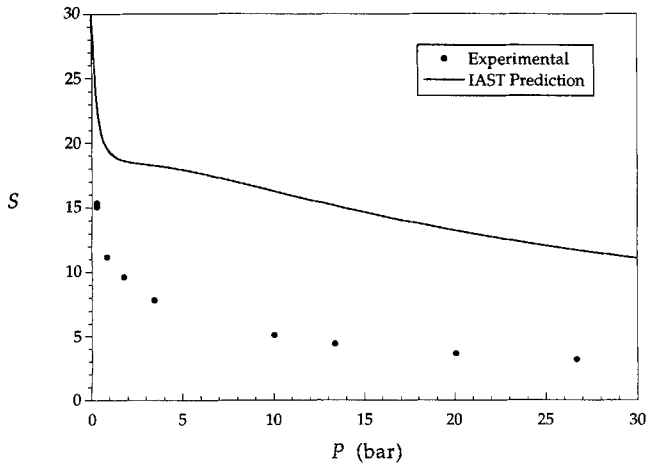

Figure 1. Experimental selectivities (points) and IAST predictions (line) for the adsorption of a 51.2% ethane, 48.8% methane mixture on BPL at T = 308.15 K.

$$Ad\pi = \sum n_i d\mu_i. \tag{2}$$

The Gibbs adsorption isotherm allows the calculation of the spreading pressure directly from the adsorption isotherm.

The ideal adsorbed solution theory (IAST) of Myers and Prausnitz (1965), which may be regarded as an industry standard, uses the concept of spreading pressure to predict multicomponent adsorption equilibria. The IAST is a thermodynamically rigorous theory based on the mixing of individual components at constant spreading pressure to form an ideal solution. In these calculations the Gibbsian concept of a single homogeneous adsorbed phase forms the basis of the multicomponent prediction.

The IAST gives accurate predictions of multicomponent equilibria for some adsorbate/adsorbent systems and is, on the whole, at least as good as other established methods (Yang, 1987; Valenzuela and Myers, 1984). However, in many cases the predictions of the IAST are unsatisfactory. Figure 1, which shows some of our experimental data for the adsorption of binary mixtures of ethane and methane on an activated carbon, along with the IAST prediction, highlights this. (The experimental method is described below.) The composition of the adsorbed phase is presented in terms of the selectivity, S, which is defined by

$$S = \frac{x_{\text{eth}}/y_{\text{eth}}}{x_{\text{meth}}/y_{\text{meth}}}. \tag{3}$$

The steep decline in selectivity with increasing pressure shown by this system is not reproduced by the IAST. It is significant that the IAST performs poorly for this mixture, which is almost an ideal solution in the bulk liquid phase. It is thus difficult to attribute the disagreement between theory and experiment to nonidealities (in the sense of deviations from Raoult's law) and it is generally accepted that nonuniformity of the adsorbed phase plays a significant role.

One source of nonuniformity is an energetically heterogeneous adsorbent surface, leading to local variations in both the extent of adsorption and the composition of the adsorbate. A second source of adsorbed-phase nonuniformity reflects the nature of the adsorption process itself. For a homogeneous surface in the Henry's law limit, where only isolated adsorbent–adsorbate interactions are significant, the IAST is exact. At higher loadings, however, adsorption occurs both on the surface itself and on already-adsorbed molecules. This effect is particularly important in microporous adsorbents. Molecules experience a different local environment depending on their location. Close to the surface, the adsorbent–adsorbate interaction is dominant, while far from the surface the adsorbate–adsorbate interactions become more important. Thus, at all but the lowest pressures, adsorbed-phase nonuniformity is inherent to the adsorption process.

In practice both contributions to adsorbate nonuniformity are likely to be present, and their relative magnitude is an open question. Efforts so far have focused on accounting for the effect of adsorbent heterogeneity. Variants of the IAST incorporating adsorbent heterogeneity have been proposed (Valenzuela et al., 1988), and these can be grouped under the heading heterogeneous ideal adsorbed solution theory (HIAST). In the HIAST, the adsorbent surface is divided into many patches, each of which is characterized by a different adsorption energy. A patch may also be regarded as an individual pore of a particular size. The IAST is applied separately to the patches, which are assumed to be independent of each other. The overall adsorbate composition is obtained by integrating over an energy distribution. Although the HIAST works well for some systems, the increase in performance over the original IAST is modest and this theory has not been widely used in practical applications of adsorption.

In this article, we pursue the idea that the second contribution, which we term "inherent" nonuniformity, makes the dominant contribution to the overall nonuniformity of the adsorbed phase, while ignoring the contribution of adsorbent heterogeneity. We present a new model for multicomponent adsorption on noncrystalline porous solids and compare the predictions of the model with experimental adsorption measurements.

The Multispace Adsorption Model

In proposing the Multispace Adsorption Model (MSAM), we have in mind noncrystalline (or only partially crystalline) adsorbents, such as carbons, silicas, and aluminas, rather than zeolites. In order to distinguish between the effects of adsorbent–adsorbate and adsorbate–adsorbate interactions in these amorphous adsorbents, the pore volume is divided into two "spaces," as shown in Figure 2. By distinguishing between the effective mechanisms of adsorption in these spaces we take into account, in an approximate way, the inherent nonuniformity of the adsorbate.

In Space I, close to the adsorbent surface, the adsorbate molecules interact strongly with the adsorbent. The molecules in Space II are further from the surface of the adsorbent; they interact with the molecules in Space I and are assumed not to interact directly with the adsorbent. The amount adsorbed in Space II depends on the occupancy of Space I. Thus, in our model, the nonuniformity of the adsorbed phase is due to the proximity or otherwise of an adsorbed molecule

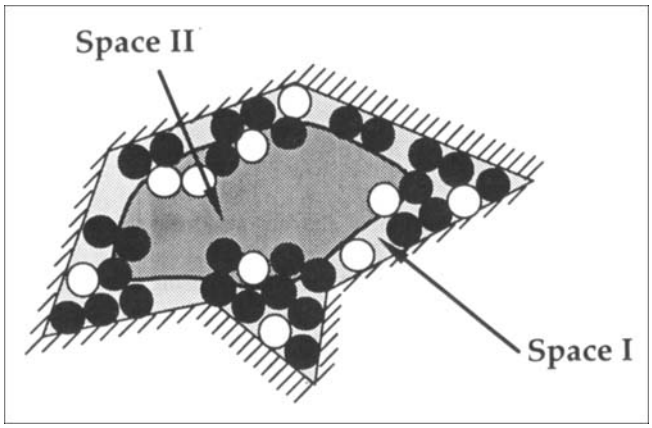

Figure 2. Schematic cross section of a pore, showing the notional division of the pore volume into Spaces I and II.

to the surface. We note that this approach can be extended to incorporate more than two spaces with, for example, molecules in the Space III interacting with those in Space II. As will be shown below, we have not found this to be necessary, as good agreement with experiment is obtained with the two-space version.

We begin by deriving a model isotherm for the adsorption of a pure species. The total adsorption of species i, n_i, is simply the sum of the number of moles adsorbed in each space:

$$n_i = n_{i,\mathrm{I}} + n_{i,\mathrm{II}} \tag{4}$$

Here, and elsewhere, the second subscript indicates the space in which adsorption occurs. The fraction of the total pore volume occupied by Space I, R, is related to the amounts adsorbed at pore filling (i.e., at infinite pressure) by

$$R = \frac{n_{i,\mathrm{I}}^{\infty}}{n_i^{\infty}} \tag{5}$$

It follows that

$$\frac{n_i}{n_i^{\infty}} = R\frac{n_{i,\mathrm{I}}}{n_{i,\mathrm{I}}^{\infty}} + (1-R)\frac{n_{i,\mathrm{II}}}{n_{i,\mathrm{II}}^{\infty}} \tag{6}$$

Adsorption in Space I is considered to be independent of Space II. We use the Langmuir isotherm to represent adsorption in Space I.

$$\frac{n_{i,\mathrm{I}}}{n_{i,\mathrm{I}}^{\infty}} = L_{i,\mathrm{I}}(P) = \frac{K_{i,\mathrm{I}}P}{1+K_{i,\mathrm{I}}P} \tag{7}$$

Here, $K_{i,\mathrm{I}}$ is the Langmuir constant for the adsorption of species i in Space I, and is also the Henry's constant for adsorption in this space. Adsorption in Space II depends on the occupancy of Space I. The molecules in Space II are considered to be adsorbed on the molecules in Space I (although physically a molecule in Space II is not necessarily in direct contact with a molecule in Space I). Effectively, the molecules in Space I are considered to constitute a "pseudoadsorbent" on which molecules in Space II adsorb. This idea, which is similar in spirit to the BET theory of adsorption, was introduced for a nonporous solid by Sircar (1985). The isotherm for Space II is obtained by assuming that if Space I were fully occupied, adsorption of component i in Space II would be described by a Langmuir isotherm. This isotherm is scaled by the fractional occupancy of Space I, $L_{i,\mathrm{I}}(P)$, to give the amount actually adsorbed in Space II:

$$\frac{n_{i,\mathrm{II}}}{n_{i,\mathrm{II}}^{\infty}} = L_{i,\mathrm{I}}(P)L_{i,\mathrm{II}}(P) \tag{8}$$

where

$$L_{i,\mathrm{II}}(P) = \frac{K_{i,\mathrm{II}}P}{1+K_{i,\mathrm{II}}P} \tag{9}$$

The overall isotherm for the adsorption of pure species i is

$$\frac{n_i}{n_i^{\infty}} = L_{i,\mathrm{I}}(P)[R+(1-R)L_{i,\mathrm{II}}(P)] \tag{10}$$

The three parameters implicitly contained within Eq. 10 ($K_{i,\mathrm{I}}$, $K_{i,\mathrm{II}}$, n_i^{∞}), are determined by fitting to pure-species isotherm data. The parameter R reflects the structure of the adsorbent and must be found separately, as will be discussed below.

The multicomponent prediction is made by applying the IAST separately to each space, using the pure species isotherms for the two spaces as inputs. The Space I calculation is straightforward, and is essentially a standard IAST calculation (Myers and Prausnitz, 1965), which may be summarized as follows. In the ideal gas in equilibrium with an ideal adsorbed solution, the partial pressure of an adsorbed component equals the product of its mole fraction in the adsorbed phase and the pressure that it would exert as a pure adsorbed species at the specified temperature and at the spreading pressure of the mixture. For Space I this may be written as:

$$p_i = Py_i = P_{i,\mathrm{I}}^{o}(\pi_{\mathrm{I}})x_{i,\mathrm{I}} \tag{11}$$

where $P_{i,\mathrm{I}}^{o}(\pi_{\mathrm{I}})$ is a standard state pressure. (This standard state pressure is the pure species pressure corresponding to adsorption in Space I only.) The spreading pressure in Space I is related to $P_{i,\mathrm{I}}^{o}$ using the Gibbs adsorption isotherm:

$$\frac{\pi_{\mathrm{I}}A}{R_gT} = \int_0^{P_{i,\mathrm{I}}^{o}} \frac{n_{i,\mathrm{I}}}{t}dt = \int_0^{P_{i,\mathrm{I}}^{o}} \frac{L_{i,\mathrm{I}}(t)\,Rn_{i,\mathrm{I}}^{\infty}}{t}dt \tag{12}$$

where t is a dummy variable of integration, and R_g is the gas constant. The composition of the adsorbate in Space I is calculated from Eq. 11 by matching the spreading pressures of each component. The amounts adsorbed of each species is given by

$$\frac{1}{\tilde{n}_{t,\mathrm{I}}} = \sum \frac{x_{i,\mathrm{I}}}{n_{i,\mathrm{I}}^{o}}, \tag{13}$$

where $n^o_{i,\mathrm{I}}$ is the number of moles of pure species i that would be adsorbed at $P^o_{i,\mathrm{I}}$, and $\tilde{n}_{t,\mathrm{I}}$ is the total number of moles adsorbed as a mixture in Space I.

In Space II we view adsorption as occurring on a pseudoadsorbent formed by Space I. Thus the Langmuir constants for Space II should reflect the fact that mixture adsorption in Space II takes place on the mixture occupying Space I, rather than on pure species i. We use the following quadratic mixing rules (which, since the Langmuir constants are also the Henry's constants for pure species adsorption, are exact within the context of this model) to calculate the effective Henry's constant for the adsorption of species i in Space II, $\tilde{K}_{i,\mathrm{II}}$:

$$K_{ij,\mathrm{II}} = K_{ji,\mathrm{II}} = \sqrt{K_{i,\mathrm{II}} K_{j,\mathrm{II}}}, \quad K_{ii,\mathrm{II}} = K_{i,\mathrm{II}} \tag{14}$$

$$\tilde{K}_{i,\mathrm{II}} = \sum_j K_{ij,\mathrm{II}} x_{j,\mathrm{I}}. \tag{15}$$

Equation 9 rewritten for mixture adsorption becomes:

$$\tilde{L}_{i,\mathrm{II}}(P) = \frac{\tilde{K}_{i,\mathrm{II}} P}{1 + \tilde{K}_{i,\mathrm{II}} P}. \tag{16}$$

The spreading pressure in Space II is calculated as follows:

$$\frac{\pi_{\mathrm{II}} A}{R_g T} = \int_0^{P^o_{i,\mathrm{II}}} \frac{n_{i,\mathrm{II}}}{t} dt = \int_0^{P^o_{i,\mathrm{II}}} \theta(t) \frac{\tilde{L}_{i,\mathrm{II}}(t)(1-R) n^\infty_{i,\mathrm{II}}}{t} dt \tag{17}$$

where θ is the fractional occupancy of Space I and $P^o_{i,\mathrm{II}}$ is the standard state pressure for Space II. The evaluation of the integral in Eq. 17 requires some discussion. First, as the IAST calculations in the two spaces are carried out at a given value of the bulk pressure P, and the pure-species isotherms are different in each space, the spreading pressures and the standard state pressures are different in the two spaces. Second, because Space I evolves with pressure, θ appears within the integral. Thus it is necessary to solve the Space I problem completely before tackling Space II. Using the IAST assumption of no area change in mixing, θ is calculated as follows:

$$\theta = \sum \frac{\tilde{n}_{i,\mathrm{I}}}{n^\infty_{i,\mathrm{I}}}, \tag{18}$$

where $\tilde{n}_{i,\mathrm{I}}$ is the predicted number of moles of species i in Space I for the mixture. The IAST reformulated for the Space II calculation yields:

$$p_i = P y_i = P^o_{i,\mathrm{II}}(\pi_{\mathrm{II}}) x_{i,\mathrm{II}} \tag{19}$$

$$\frac{1}{\tilde{n}_{t,\mathrm{II}}} = \sum \frac{x_{i,\mathrm{II}}}{n^o_{i,\mathrm{II}}}. \tag{20}$$

This allows the prediction of the composition and amounts of each species adsorbed in Space II.

Finally, the total number of moles adsorbed of each species in the mixture is given by summing over the two spaces:

$$\tilde{n}_i = \tilde{n}_{i,\mathrm{I}} + \tilde{n}_{i,\mathrm{II}} \tag{21}$$

and

$$\tilde{n}_t = \tilde{n}_{t,\mathrm{I}} + \tilde{n}_{t,\mathrm{II}}. \tag{22}$$

The overall composition of the adsorbed phase follows directly from Eqs. 21 and 22.

Although we have derived the MSAM using the Langmuir isotherm to describe pure-species adsorption in each space, other isotherms may be used. The Langmuir isotherm is strictly speaking a model for monolayer adsorption on fixed sites, and does not account for the compressibility of the adsorbate. In the remainder of this section we consider a different isotherm equation that is more appropriate to mobile adsorption.

Jensen and Seaton (1995) have proposed a modified form of the Toth equation (Toth, 1962) for adsorption in microporous solids:

$$n(P) = KP\left[1 + \left(\frac{KP}{a(1+\kappa P)}\right)^c\right]^{-1/c}, \tag{23}$$

where K is the Henry's constant, κ is the compressibility of the adsorbed phase, and a is a measure of the capacity of the adsorbent. The slope of the isotherm at high pressure is given by κa. The exponent c is purely empirical. In this work we use a simplification of this isotherm for $c = 1$:

$$n(P) = \frac{aKP + \kappa a K P^2}{a + (K + \kappa a) P}. \tag{24}$$

Equation 24 reduces to the Langmuir isotherm for $\kappa = 0$.

Applying this isotherm to the MSAM model gives the following equations for the pure-species isotherms in Spaces I and II, respectively:

$$\frac{n_{i,\mathrm{I}}}{R a_i} \equiv T_{i,\mathrm{I}}(P) = \frac{K_{i,\mathrm{I}} P(1+\kappa_i P)}{R a_i + (K_{i,\mathrm{I}} + R a_i \kappa_i) P} \tag{25}$$

$$\frac{n_{i,\mathrm{II}}}{(1-R) a_i} \equiv T_{i,\mathrm{II}}(P) = \frac{K_{i,\mathrm{II}} P(1+\kappa_i P)}{(1-R) a_i + (K_{i,\mathrm{II}} + (1-R) a_i \kappa_i) P}. \tag{26}$$

Because the isotherm of Jensen and Seaton (which we designate the "modified Toth" isotherm) allows for the compressibility of the adsorbed phase, the concept of an extent of adsorption at infinite pressure is inapplicable; we show this explicitly by using the notation a_i instead of n^∞_i as a measure of capacity. As a consequence, $T_{i,\mathrm{I}}(P)$ can strictly no longer be identified physically as the fractional occupancy of Space I. However this interpretation is reasonable at pressures characteristic of practical applications of adsorption, for example, adsorptive separations. We make the physically plausible approximation that the compressibility of pure species i is equal in both spaces.

The overall isotherm for the pure species is now written as

$$\frac{n_i}{a_i} = T_{i,I}(P)[R + (1-R)T_{i,II}(P)]. \qquad (27)$$

Equation 27 contains one more parameter, κ, than the Langmuir-based pure-species isotherm.

Experimental Studies

All of the single-component and binary (ethane/methane) adsorption data presented in Figure 1, and Figures 4–14 were measured in our laboratory using a custom-built apparatus. The apparatus, which is shown in Figure 3, is capable of both static volumetric (for pure species) and flowthrough (for mixtures) measurements. Measurements were carried out at 308.15, 333.15 and 373.15 K and pressures from several torr to 25,000 torr (about 33 atm). In the case of the binary mixtures, gas-phase methane concentrations of 48.8 and 75.2 mol % were used.

For single-component adsorption measurements the static volumetric technique was used. In this technique, the pressure, volume, and temperature of the gas are measured before and after it contacts the adsorbent; these data are then used to calculate the extent of adsorption using the gas equation of state. This procedure is carried out first at the lowest pressure of interest and then repeated at progressively higher pressures. The pressure is measured using either of two MKS Baratron capacitance pressure gauges, models 127A and 122A covering ranges of 0.1 to 1,000 torr and 100 to 25,000 torr, respectively, and a model PDR-C-2C digital readout. The pressure measurements are accurate to within 0.15% of the reading.

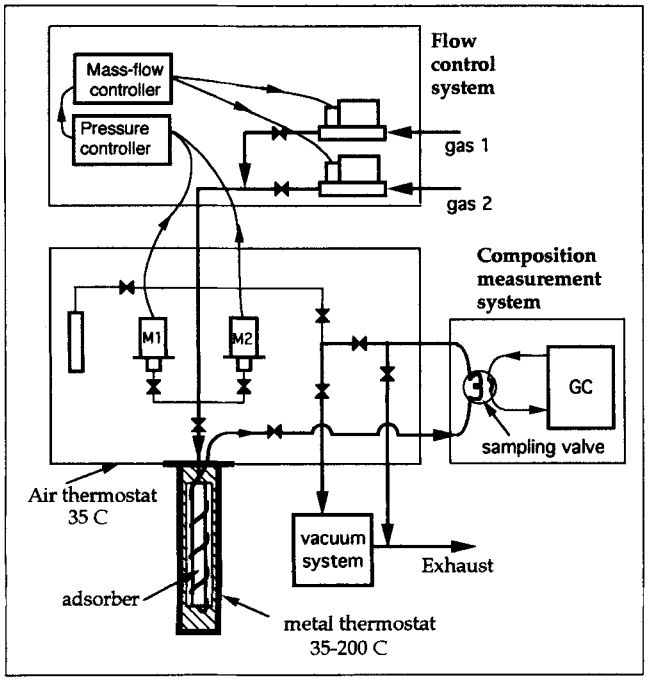

Figure 3. Adsorption apparatus.

M1, M2: Baratron pressure transducers. GC: gas chromatograph. See text for description.

The reference volume, pressure gauges, and stainless-steel plumbing are inside an air thermostat, controlled at 35°C using convection heating and four temperature gauges. The stainless-steel adsorber was held at the adsorption temperature within a second thermostat. Our apparatus is capable of operating in the temperature range 35°C to 200°C. The thermostat is a removable aluminum cylinder with a temperature sensor and a heater mounted on its external surface. The aluminum cylinder is wrapped in insulating cloth and inserted in a glass Dewar flask to avoid heat losses to the environment. The adsorber is connected to the volumetric system by stainless-steel capillary tubing, which is coiled inside the aluminum cylinder to allow thermal equilibration of the gas flow before it enters the adsorber. The temperature in each of the thermostats is controlled to within 0.2 K by an Omega model CN8500 PID controller with digital display and Omega model 100W platinum resistance sensors.

The dead volumes were calibrated by helium expansion from the reference volume. For this reason, the adsorption is measured in the Gibbs excess, rather than the absolute, sense. The accuracy of each pure-species adsorption point is estimated to be about 1%.

For *binary measurements* we used an open flow system (Reich et al., 1980; Talu and Zweibel, 1986) built onto the single-component stage. This arrangement allows the measurement of mixture adsorption at a specified gas-phase pressure and composition, which is the most useful for analysis purposes.

A specified gas-phase pressure and composition is maintained using an MKS flow control setup. A PI pressure controller, model 250C, receives an input signal from the pressure readout electronics. The output signal of the pressure controller is used as an external set point for the two-channel flow-control system to produce the gas flow necessary to achieve the required pressure. The flow-control system itself consists of two mass flow controllers, model 1261C, and a digital flow-rate/readout/setpoint source, model 247C. The flow rate in one of the channels is changed with respect to the pressure signal as a "master" and in the other channel as "slave." In this manner, the composition of the flowing gas mixture is insensitive to small downstream pressure oscillations. The total flow rate was adjusted to about 200 cm^3/min for each given pressure using a needle valve located downstream of the adsorber.

Samples were taken from the adsorber effluent stream via a six-port sampling valve, and then routed to a Hewlett-Packard model 5880A gas chromatograph fitted with a packed column and a flame ionization detector.

A steady composition downstream of the adsorber (indicating equilibrium) was usually attained in 1 to 2 h; at this point, the adsorber bypass was gradually opened to eliminate the flow-induced pressure drop across the adsorber. Once equilibrium was restored, the adsorber was isolated. The remaining volumes of the system were outgassed, and the adsorbate was transferred to the reference volume by cooling the latter with liquid nitrogen while heating the adsorber at the temperature of the initial outgassing. In this way essentially all the adsorbed gas could be desorbed in about 4 h.

Following desorption, the mixture was allowed to expand into the thermostatted nonadsorber volumes of the system, and was held overnight to ensure adequate mixing. Finally,

the pressure and composition of the desorbed gas (i.e., the former adsorbed phase) were measured, and these data were used to compute the amount and composition of the adsorbed phase. In the binary adsorption experiments, the accuracy of the total amount adsorbed is estimated at about 3%. The composition measurements are estimated to be accurate to within 0.5%.

Materials

About 20 g of the microporous carbon (BPL 6×16, Calgon Carbon Corporation, Pittsburgh) were outgassed at 10 μm of mercury pressure and 100°C for 24 h in a glass ampoule. Following this treatment, the ampoule was sealed off, weighed, carefully broken, and the slivers were weighed again. The mass of the outgassed adsorbent, which was used in all subsequent calculations, was supplied as the difference between the two balance readings. The adsorbent was placed into the metal adsorber and thermostat and outgassed at the preceding conditions. This same adsorbent sample was used in all of the experiments reported here.

The methane and ethane gases supplied by National Compressed Gases, Inc., had quoted purity of better than 99.97% and were used without further purification.

Results

In this section, we predict multicomponent adsorption equilibrium using the MSAM, with experimental pure-species isotherms as an input, and compare the predictions with experimental multicomponent data. In addition to our own data, we use the data sets of Reich et al. (1980) and Szepesy and Illes (1964), which are widely used in the testing of adsorption thermodynamic models.

We implemented the MSAM in C, on a Sun SparcStation 10. A single MSAM calculation requires of the order of 10^{-3} s. MSAM calculations are thus fast enough to be carried out repeatedly within a simulation of, for example, an adsorptive separation process, using either a Unix workstation or a modern PC.

Figures 4 to 6 show our data for the adsorption of pure methane and ethane on BPL carbon. The data are correlated using Eq. 27 (the MSAM isotherm based on the modified Toth isotherm), giving a good fit. The MSAM multicomponent predictions require as inputs $K_{i,\mathrm{I}}$, $K_{i,\mathrm{II}}$, a_i, κ_i for each species, and the structural parameter R. The parameter R, which is a property only of the particular adsorbent, and is

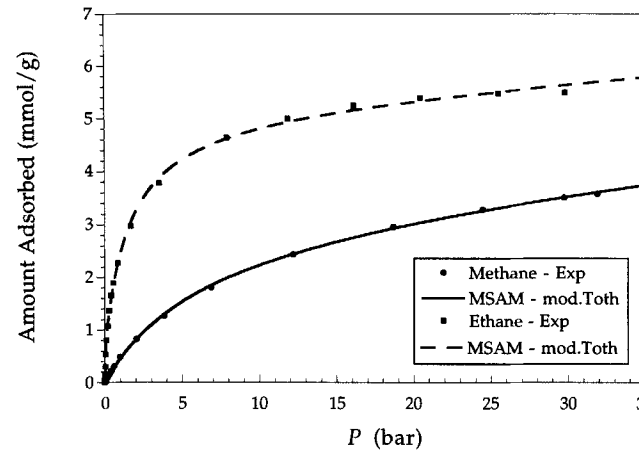

Figure 5. Fits of the modified Toth MSAM with $R = 0.2$ (lines) to the pure-methane and pure-ethane adsorption data (points) on BPL activated carbon at $T = 333.15$ K.

Fitted parameter values are as follows: methane: $K_{\mathrm{I}} = 0.5167$ mmol·g^{-1}·bar^{-1}, $K_{\mathrm{II}} = 0.0280$ mmol·g^{-1}·bar^{-1}, $a = 17.421$ mmol·g^{-1}, $\kappa = 0.00234$ bar^{-1}; ethane: $K_{\mathrm{I}} = 12.441$ mmol·g^{-1}·bar^{-1}, $K_{\mathrm{II}} = 2.5620$ mmol·g^{-1}·bar^{-1}, $a = 5.2713$ mmol·g^{-1}, $\kappa = 0.00222$ bar^{-1}.

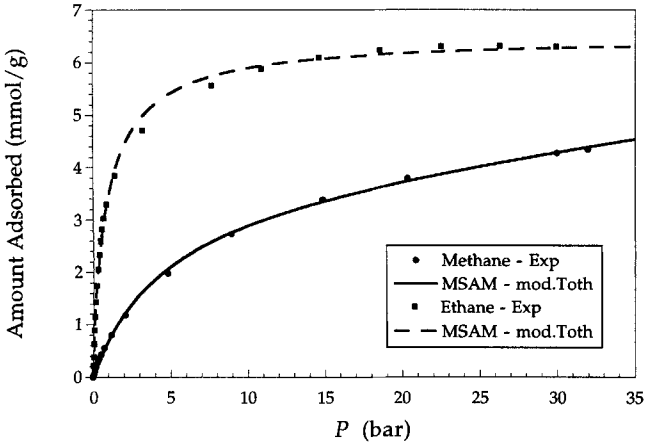

Figure 4. Fits of the modified Toth MSAM with $R = 0.2$ (lines) to the pure-methane and pure-ethane adsorption data (points) on BPL activated carbon at $T = 308.15$ K.

Fitted parameter values are as follows: methane: $K_{\mathrm{I}} = 0.8610$ mmol·g^{-1}·bar^{-1}, $K_{\mathrm{II}} = 0.0281$ mmol·g^{-1}·bar^{-1}, $a = 19.048$ mmol·g^{-1}, $\kappa = 0.00255$ bar^{-1}; ethane: $K_{\mathrm{I}} = 28.398$ mmol·g^{-1}·bar^{-1}, $K_{\mathrm{II}} = 4.2838$ mmol·g^{-1}·bar^{-1}, $a = 6.4878$ mmol·g^{-1}, $\kappa = 0.0000$ bar^{-1}.

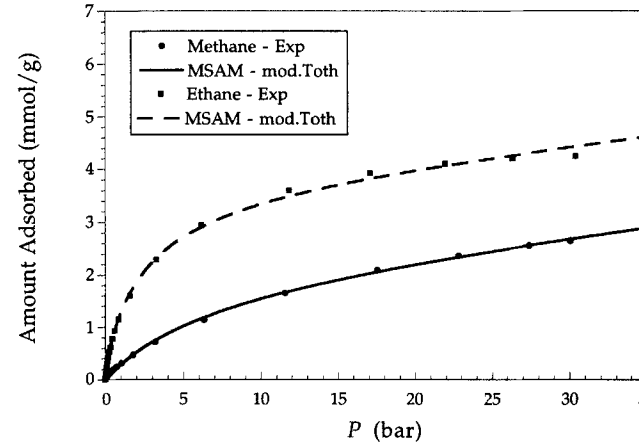

Figure 6. Fits of the modified Toth MSAM with $R = 0.2$ (lines) to the pure-methane and pure-ethane adsorption data (points) on BPL activated carbon at $T = 373.15$ K.

Fitted parameter values are as follows: methane: $K_{\mathrm{I}} = 0.3243$ mmol·g^{-1}·bar^{-1}, $K_{\mathrm{II}} = 0.0258$ mmol·g^{-1}·bar^{-1}, $a = 11.837$ mmol·g^{-1}, $\kappa = 0.00334$ bar^{-1}; ethane: $K_{\mathrm{I}} = 3.2512$ mmol·g^{-1}·bar^{-1}, $K_{\mathrm{II}} = 1.1027$ mmol·g^{-1}·bar^{-1}, $a = 3.8884$ mmol·g^{-1}, $\kappa = 0.00427$ bar^{-1}.

independent of temperature and the nature of the adsorbing mixture, is chosen by adjustment to allow MSAM to fit a limited amount of mixture data for an arbitrary binary mixture and temperature. In Figures 4 to 6 we have chosen $R = 0.2$, based on a comparison with limited mixture data. (The implications and details of the choice of R, which is crucial to the performance of MSAM, are addressed below.) To ensure that the remaining parameters maintained the physical basis intended them, the value of the compressibility, κ, was estimated from the gradient between the high pressure data points. Then the three remaining parameters were fitted to all the data points using a least-mean-squares routine. A similar approach was used to estimate the parameters of the MSAM model based on the Langmuir isotherm, except that there is no parameter κ.

The effect of the parameter R on selectivity predictions for both versions of the MSAM model discussed is shown in Figures 7 and 8. Predicted selectivities for a 0.48 ethane–methane mixture on BPL at 308.15 K, using the correlations of our pure-species data as inputs, are plotted for various values of R. Also shown in these figures are the experimental selectivity data for this mixture, as well as the IAST prediction for comparison. For both Langmuir and modified Toth MSAM, the predicted selectivity curve is a strong function of R. The limit $R = 1$ corresponds to IAST. The IAST calculations carried out in this work use, as the single component isotherm, the pure-component form of the MSAM model. This ensures a fair comparison, in the sense that the IAST and the MSAM predictions will then concur at low pressure, as they must, when only the interactions between molecules and the surface should affect the adsorption behavior. For both MSAM and IAST, the selectivity reduces at low pressure to the ratio of the Henry's constants (i.e., $K_{i,I}$, in the case of MSAM).

Figure 7 shows the performance of the MSAM based on the Langmuir isotherm. Performance is significantly better than IAST for all values of R shown. The improvement is most impressive at low pressures; at higher pressures, although performing better than IAS, the MSAM prediction fails to capture the continuing decline in the selectivity with increasing pressure. This is a consequence of using the Langmuir isotherm, which on extrapolation simply approaches the total pore-filling value and becomes insensitive to pressure. Figure 8 shows the performance of the MSAM based on the modified Toth isotherm. $R = 0.2$ yields excellent agreement with experimental selectivities over the entire pressure range.

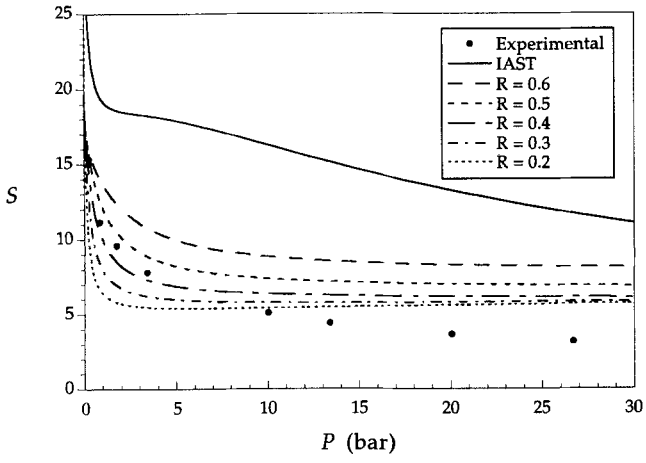

Figure 7. Experimental selectivities (points), IAST predictions (solid line), and Langmuir MSAM predictions with various R values (broken lines) for the adsorption of a 51.2% ethane, 48.8% methane mixture on BPL at T=308.15 K.

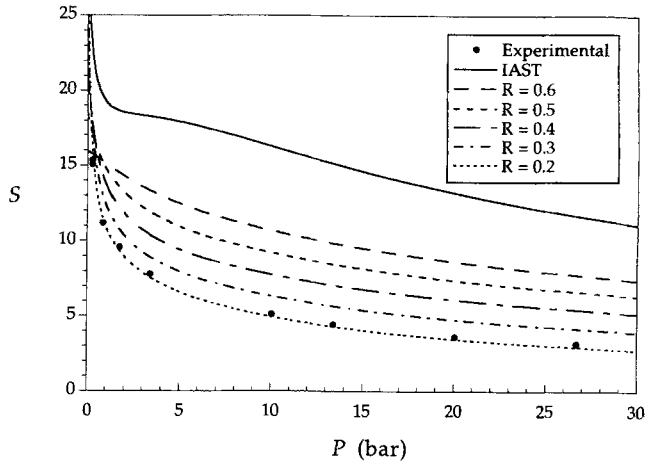

Figure 8. Experimental selectivities (points), IAST predictions (solid line), and modified Toth MSAM predictions with various R values (broken lines) for the adsorption of a 51.2% ethane, 48.8% methane mixture on BPL at T=308.15 K.

For the present purpose of evaluating the performance of the theory, and in particular to test the assumption that R is indeed only a characteristic of the adsorbent structure (for a given elementary "space" isotherm), we repeat the MSAM predictions at different compositions and temperatures. Based on the observations in Figures 7 and 8, the values of R that give roughly optimal performance for the BPL carbon are $R = 0.4$ for the Langmuir-based MSAM and $R = 0.2$ for the modified Toth MSAM. Figures 9–14 show selectivity curves predicted using the MSAM at two bulk compositions (48% and 75% methane) and three temperatures (301, 333, and 373 K), along with our experimental data taken at pressures up to 27 bar. Again IAST predictions are shown for comparison. The MSAM predictions are in excellent agreement with the experimental results over the wide range of conditions studied. While both the MSAM and the IAST give good predictions at very low pressures, the IAST curve declines only gradually with increasing pressure and deviates significantly from the experimental data. The MSAM, on the other hand, is in excellent agreement with experiment over the whole pressure range studied.

In a practical application of multicomponent adsorption thermodynamics, it is unlikely that much multicomponent data would be available, in which case the estimation of R in this way would not be possible. However, our experience suggests that a satisfactory value of R can in practice be obtained from only very limited mixture data; we return to this point in the Discussion section.

Reich et al. (1980) studied the adsorption of pure species and mixtures on BPL carbon (nominally the same carbon as

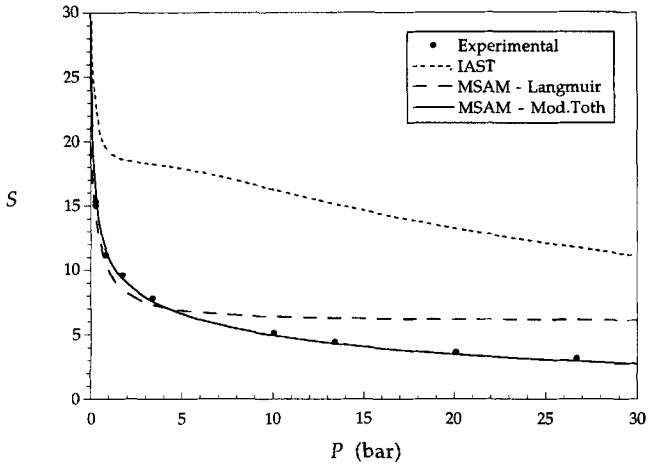

Figure 9. Experimental selectivities (points), and predictions of IAST (short dashes), Langmuir MSAM with $R = 0.4$ (long dashes), and modified Toth MSAM with $R = 0.2$ (solid line), for the adsorption of a 51.2% ethane, 48.8% methane mixture on BPL at $T = 308.15$ K.

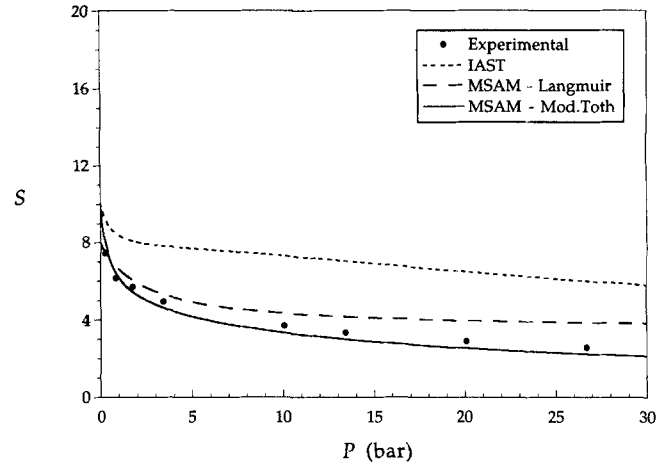

Figure 11. Experimental selectivities (points), and predictions of IAST (short dashes), Langmuir MSAM with $R = 0.4$ (long dashes), and modified Toth MSAM with $R = 0.2$ (solid line), for the adsorption of a 51.2% ethane, 48.8% methane mixture on BPL at $T = 373.15$ K.

we used in our experiments). They reported binary data for ethane–methane and ethylene–methane, and for the ternary mixture ethylene–ethane–methane, along with data for the adsorption of the pure species involved. In applying the MSAM to the data of Reich et al., we correlated the pure species data using the same values of R used in our work (in accordance with our postulate that R is a function only of adsorbate structure). Figures 15 and 16 are examples of the performance of the MSAM in predicting the multicomponent data of Reich et al. (1980). As before, MSAM is seen to perform significantly better than the IAST over the entire pressure range of the binary data, while the IAST is accurate only at very low pressures. For brevity, we show only a limited comparison with the data of Reich et al.; the MSAM performs similarly (sometimes better and sometimes worse) for all the binary data at 301.15 K reported by those workers. Neither IAST nor MSAM performed well with the 212 K data measured by Reich et al., with errors being greatest at the low pressures. Since both these models are exact in the Henry's Law region, we feel the poor performance simply emphasizes the importance of the low-pressure adsorption data and does not reflect failings in the MSAM.

The predictions in Figures 15 and 16 could have been further improved by using $R = 0.5$ (instead of 0.4) for the Langmuir MSAM, and $R = 0.3$ (instead of 0.2) for the modified Toth MSAM calculation. We chose instead to keep R con-

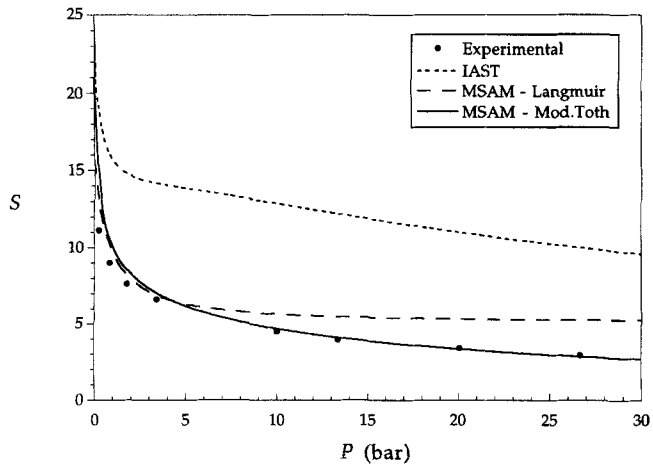

Figure 10. Experimental selectivities (points), and predictions of IAST (short dashes), Langmuir MSAM with $R = 0.4$ (long dashes), and modified Toth MSAM with $R = 0.2$ (solid line), for the adsorption of a 51.2% ethane, 48.8% methane mixture on BPL at $T = 333.15$ K.

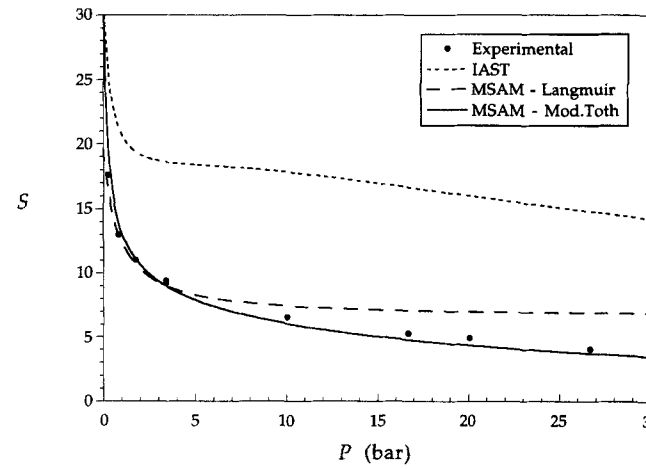

Figure 12. Experimental selectivities (points), and predictions of IAST (short dashes), Langmuir MSAM with $R = 0.4$ (long dashes), and modified Toth MSAM with $R = 0.2$ (solid line), for the adsorption of a 25% ethane, 75% methane mixture on BPL at $T = 308.15$ K.

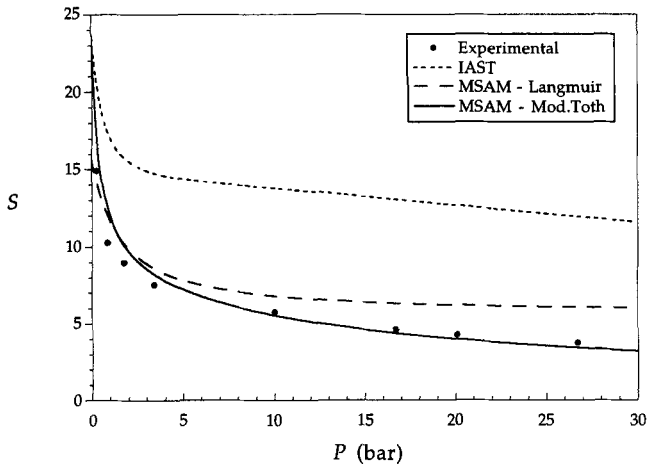

Figure 13. Experimental selectivities (points), and predictions of IAST (short dashes), Langmuir MSAM with $R = 0.4$ (long dashes), and modified Toth MSAM with $R = 0.2$ (solid line), for the adsorption of a 25% ethane, 75% methane mixture on BPL at $T = 333.15$ K.

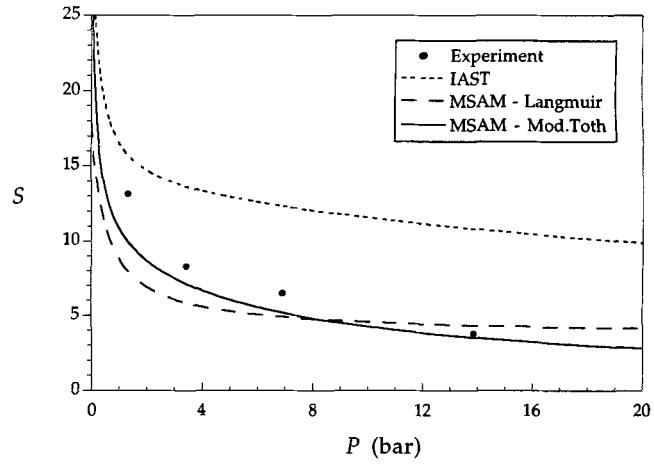

Figure 15. Experimental selectivities (points) of Reich et al. (1980), and predictions of IAST (short dashes), Langmuir MSAM with $R = 0.4$ (long dashes), and modified Toth MSAM with $R = 0.2$ (solid line), for the adsorption of a 50.1% ethane, 49.9% methane mixture on BPL at $T = 301.4$ K.

stant for the following reasons. First, we note that two batches of adsorbent produced about 15 years apart are likely to have significant physical (i.e., structural, as opposed to chemical) differences; indeed, we find modest differences between our adsorption measurements and those of Reich et al., especially for pure ethane. Second, our pure component data at $T = 308.15$ K extends down to 0.01 bar in the case of ethane and 0.002 bar for the case of methane. In contrast, the measurements of Reich et al. at $T = 301.15$ K only go as low as 0.31 bar in the case of ethane and 0.72 bar in the case of methane. These two factors should be taken into consideration when noting that the roughly optimal value of R seems to have changed slightly. However, as the MSAM is an engineering thermodynamic model, it must in practice be able to accommodate these factors, without refitting R; for this reason we have retained the value of R obtained from our own measurements for the calculations of Figures 15 and 16. Despite this, the MSAM predictions are still reasonably accurate, and much better than those of IAST.

Figure 17 shows the performance of the MSAM, and for comparison the IAST, in predicting ternary data measured by Reich et al. (1980). The modified Toth isotherm (with $R = 0.2$ as before) was used to correlate the pure-species data. Agreement between the MSAM and experiment is noticeably

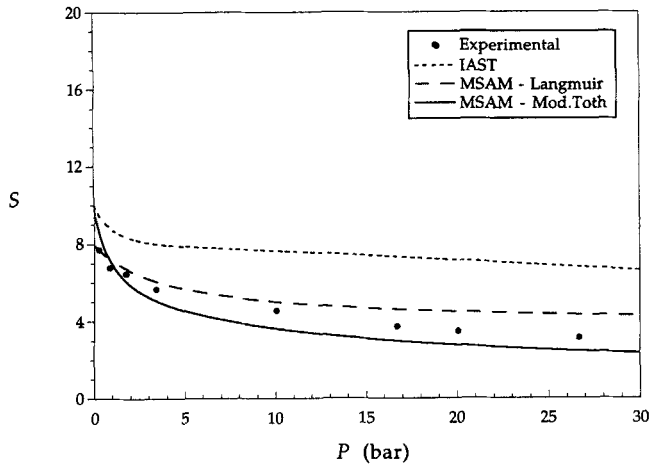

Figure 14. Experimental selectivities (points), and predictions of IAST (short dashes), Langmuir MSAM with $R = 0.4$ (long dashes), and modified Toth MSAM with $R = 0.2$ (solid line), for the adsorption of a 25% ethane, 75% methane mixture on BPL at $T = 373.15$ K.

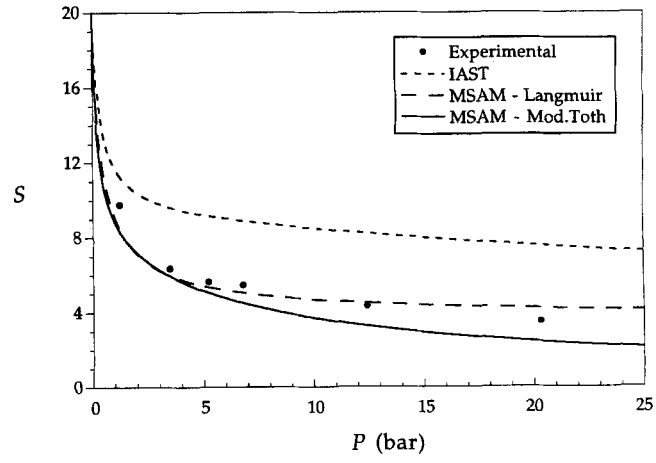

Figure 16. Experimental selectivities (points) of Reich et al. (1980), and predictions of IAST (short dashes), Langmuir MSAM with $R = 0.4$ (long dashes), and modified Toth MSAM with $R = 0.2$ (solid line), for the adsorption of a 46.4% ethylene, 53.6% methane mixture on BPL at $T = 301.4$ K.

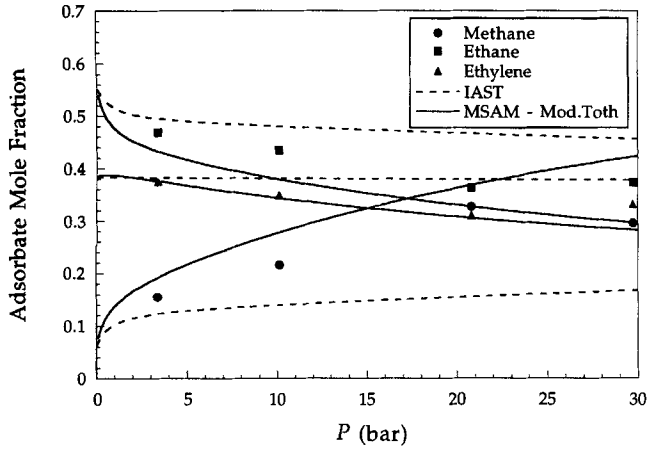

Figure 17. Ternary adsorption data (points) of Reich et al. (1980), and predictions of IAST (dashes) and modified Toth MSAM with $R = 0.2$ (solid line), for a 0.624, 0.174, 0.202 mixture of methane, ethane, ethylene on BPL at $T = 301.4$ K.

poorer than for the binary data, but is still good, and overall the MSAM performs much better than the IAST. As for the binary systems, the MSAM performs even better with the value of R optimized for the adsorbent of Reich et al. (i.e., $R = 0.3$).

We have also applied the MSAM to the data of Szepesy and Illes (1964). Figure 18 shows the comparison of Langmuir MSAM ($R = 0.8$) and IAST for the adsorption of ethane and propane on active carbon Nuxit-AL at atmospheric pressure. Both MSAM and IAST were found to perform well on this and other systems considered by Szepesy and Illes. This agrees with our expectation that both IAS and MSAM should perform similarly at low pressures.

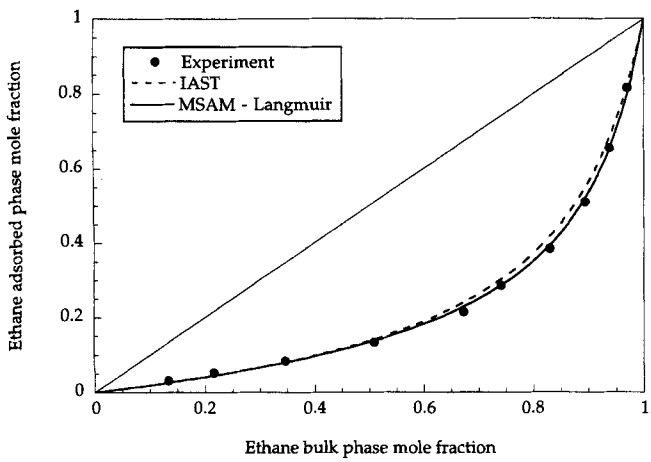

Figure 18. Binary adsorption data of Szepesy and Illes (1963), and predictions of IAST (dashes) and Langmuir MSAM with $R = 0.8$ (solid line), for an ethane–propane mixture on Nuxit AL activated carbon at $T = 293.15$ K.

Discussion

The aim of this work was to develop a new engineering model for multicomponent adsorption equilibrium. We have demonstrated that the MSAM gives a good description of extensive multicomponent adsorption data, measured in an academic environment. Industrial uses in process design are more demanding. In this section we consider the issues of experimental inputs and the choice of parameters that are important in an industrial environment, and give recommendations for the most effective use to the MSAM. We then go on to discuss some conceptual issues that arise in the construction of the MSAM.

We focus first on the experimental inputs to the MSAM. In the previous section, we used both the Langmuir isotherm and the modified Toth isotherm to correlate pure-species data (by Eqs. 10 and 27, respectively). In general the modified Toth isotherm was found to yield a superior prediction of multicomponent behavior over the entire pressure range. The reason for the enhanced performance is the inclusion of the compressibility, κ in the isotherm equation, giving the isotherm fit greater flexibility. However, the application of the modified Toth isotherm is problematical where the pure-species data do not extend to a sufficiently high pressure that the isotherm has approximately "flattened out." In such a case, the high-pressure region of the isotherm cannot be identified with the compression of the adsorbate and no physical meaning can be attached to the value of κ obtained by fitting the modified Toth isotherm to the pure component data. In practice, the fitted value of κ for such isotherms is often unreasonably high, causing erroneous multicomponent predictions at high pressure, and the Langmuir isotherm should be used in preference.

Next we consider the choice of the parameter R. In the previous section, we chose R to give an approximately optimal representation of multicomponent data over a range of pressures for a single system (see Figure 8). Because of the high cost of multicomponent adsorption measurements, the use of mixture data must be minimized in an industrial application. Fortunately, it seems that a single, carefully chosen mixture point may be enough to fix R. Good agreement with experiment is guaranteed at low pressure, as the MSAM (and indeed the IAST) are exact in the limit of zero pressure; in this limit, the selectivity is simply the ratio of the Henry's constants. In terms of binary adsorption, the main effect of R is to determine how rapidly the selectivity deviates from the Henry's law limit. Thus, our experience suggests that a single data point measured at high pressure, for any binary pair, is enough to obtain a reasonable value of R. Ideally, this measurement should be made near the lower end of the temperature range of interest, as the binary selectivity is a stronger function of pressure at lower temperatures. Consider Figure 8. Adjusting R has the effect of shifting the value of the high-pressure selectivity up or down. Note that the actual shape of the curve in this region barely changes, each curve remaining approximately parallel. This means that any of the higher pressure selectivity points could be used with equal success to estimate R. Indeed any of the high-pressure points in Figures 9 to 16 could be used in this way to get a good estimate of R. We emphasize that in the MSAM R is a property of the adsorbent alone and is in no sense a binary interaction parameter of the type found in equations of state. In

fact, for all the predictions shown in this article *regardless of the temperature or adsorbed phase identity and composition, the same value of R was used throughout for a given adsorbent.*

Throughout this article we have referred to the MSAM calculations, like those of IAST, as "predictions." As the MSAM requires limited binary data to determine the parameter R for the adsorbent of interest, its mode of prediction is different from that of IAST, and other methods that require only pure-component experimental inputs. In the sense that the MSAM can be used to calculate adsorption equilibrium at temperatures, pressures, and compositions far from the conditions that were used to fix R, and for different adsorbate mixtures, the MSAM functions as a predictive method. However, as the predictions are of the same character as one of the experimental inputs (i.e., multicomponent equilibrium data), it is also possible to view the MSAM as a correlative method, albeit one of very great scope where a single, physically based parameter allows the correlation of multicomponent adsorption data for a range of adsorbate mixtures and for widely varying conditions.

Finally, we point out that there are elements of inconsistency in our model, stemming from the fact that a "space" is neither a two-dimensional layer nor a distinct phase, but has something of the character of each. Our treatment of pure-species adsorption is reminiscent of multilayer adsorption; we have the atomistic picture of molecules in Space II adsorbing (in some loose sense) on molecules in Space I. On the other hand, the mixture calculation treats the spaces as distinct pseudophases, both of which are in equilibrium with the bulk gas. Clearly, in a microporous solid where pores are of molecular dimensions, the identification of physical pore volume fractions in which certain types of interaction occur is somewhat arbitrary. It is perhaps more realistic to regard the MSAM as simply a means of recognizing that both the wall potential and the cumulative potential of adsorbed molecules contribute to establishing an adsorbed phase, and that their relative magnitudes vary with location in the pore.

Additionally, in the MSAM adsorption in Space II depends on adsorption in Space I but not *vice versa*, whereas in reality the interaction is two-way. Furthermore, the spreading pressures are different in Spaces I and II, implying the existence of an interfacial tension between the two spaces. For these reasons, we regard the physical basis of the MSAM as qualitatively descriptive, rather than mechanistic. The MSAM is intended as a practical engineering approach, rather than a fundamental description of multicomponent adsorption equilibrium; in that role it is extremely successful.

Acknowledgments

CRCJ acknowledges a scholarship from Trinity College, Cambridge. This work is supported in part by the U.S. National Science Foundation through grant CTS-9215604.

Literature Cited

Cracknell, R. F., and D. Nicholson, "Adsorption of Gas Mixtures on Solid Surfaces, Theory and Computer Simulation," *Adsorption*, **1**, 7 (1995).

Jensen, C. R. C., and N. A. Seaton, "An Isotherm Equation for Adsorption to High Pressures in Microporous Solids," *Langmuir*, submitted (1995).

Myers, A. L., and J. M. Prausnitz, "Thermodynamics of Mixed-Gas Adsorption," *AIChE J.*, **11**, 121 (1965).

Reich, R., W. T. Zeigler, and K. A. Rogers, "Adsorption of Methane, Ethane and Ethylene Gases and Their Binary and Ternary Mixtures and Carbon Dioxide on Activated Carbon at 212–301 K and Pressures to 35 atm," *Ind. Eng. Chem. Proc. Des. Dev.*, **19**, 336 (1980).

Sircar, S., "New Isotherm for Multilayer Adsorption of Vapours on Non-porous Adsorbents," *Adsorp. Sci. Technol.*, **2**, 23 (1985).

Szepesy, L., and V. Illes, "Adsorption of Gases and Gas Mixtures I, III," *Acta Chim. Hung.*, **35**, 37, 345 (1964).

Talu, O., and I. Zwiebel, "Multicomponent Adsorption of Non-ideal Mixtures," *AIChE J.*, **32**, 1263 (1986).

Toth, J., "Gas-(Dampf-) Adsorption an Festen Oberflächen Inhomogener Aktivität, III," *Acta Chim. Hung*, **32**, 39 (1962).

Valenzuela, D. P., and A. L. Myers, "Gas Adsorption Equilibria," *Sep. Pur. Methods*, **13**, 152 (1984).

Valenzuela, D. P., A. L. Myers, O. Talu, and I. Zwiebel, "Adsorption of Gas Mixtures: Effect of Energetic Heterogeneity," *AIChE J.*, **34**, 397 (1988).

Yang, R. T., *Gas Separation by Adsorption Processes*, Butterworths, Stoneham, MA (1987).

Manuscript received Sept. 13, 1995, and revision received Mar. 1, 1996.